



PII: S0017-9310(97)00194-4

Short ducts consisting of cylindrical segments and their convective mass/heat transfer, pressure drop and performance analysis

B. BIENIASZ

Thermodynamics Department, Rzeszów University of Technology, ul. W. Pola 2, 35-959 Rzeszów,
PO Box 85, Poland

(Received 15 March 1994 and in final form 17 June 1997)

Abstract—The effect of turbulence stimulation caused by dividing a short duct into seven cylindrical segments and setting them in three different arrays at one value of displacement ratio was studied by the use of the electrolytic technique. The inlet of the duct was connected to the plenum with a diffuser causing a non-developed flow in the duct. One value of contraction ratio between the plenum and the tested duct was in use. Schmidt number was 1590. Mean values of the mass/heat transfer coefficient for each segment and the friction losses for the whole ducts were measured for Reynolds numbers spanning the range 7600–44 200. Correlations on the mean Chilton–Colburn coefficient were stated for the whole duct of three types. Performance analysis of the ducts was done at equal surface area for two common cases of equal flowrate and pumping power. The results might be used, e.g. in the design of turbine blade cooling channels and of some highly effective shell-and-tube heat exchangers. © 1997 Elsevier Science Ltd.

INTRODUCTION

There exists a great, continuous demand for convection mass/heat transfer data which is useful in the design calculations of short ducts applied in cooling, as a rule. Different means of turbulence stimulation of the flow in the duct cause intensification of the processes. The flow and mass/heat transfer processes are very complicated in these conditions, and that is why the experimental approach in research prevails.

It is the purpose of this paper to report on the results of experimental investigations on convective mass/heat transfer and friction losses for the flow through three different in-series assemblies of short tubes. All ducts consisted of seven identical, mutually-displaced cylindrical segments and were fed from a plenum-like volume. It was seen that both the entry effects and turbulence, caused by repeatedly occurring lens-like contractions and segment displacements, will cause a distinct transfer process intensification. This case does not appear to have been investigated before. There are a few previous works related to the subject.

Sparrow and Molki [1] determined local mass/heat transfer coefficients in a circular tube whose inlet was either built into a large wall or was supported, being in free space. The sharp-edged inlet induced a flow separation, causing a reattachment to occur just downstream of the inlet, which influenced the exchange process in the thermal entrance region. The results show the regions of enhanced values of local mass/heat transfer coefficients for both cases.

Dutra *et al.* [2] investigated the distribution of the mass/heat transfer coefficient for the flow in a four-

cups channel which, in the presence of the baffle, created a plenum-like space upstream of the inlet, thus ensuring the abrupt inlet condition. The mass transfer experiments were made for turbulent flow.

Sparrow and Cur [3] studied the effects of flow maldistribution caused by partial blockage of the inlet of a flat rectangular duct. They measured local mass/heat transfer coefficients on the principal walls, pressure distribution along the duct and a flow pattern which was visualized by the oil-lampblack technique. They found, from the local data, that spanwise-average heat transfer coefficients were enhanced in the downstream part of the duct due to the flow maldistribution.

Goldstein and Sparrow [4] determined the local and average transfer characteristics for flow in a corrugated channel. They measured a distribution of the mass transfer coefficient both in spanwise and streamwise directions. They stated that the average coefficient was nearly three times greater than that in the case of a smooth wall channel.

Souza Mendes and Sparrow [5] investigated a convective exchange process in a tube consisting of conical modules placed end to end. They determined the entrance region and fully-developed mass/heat transfer coefficients, pressure distributions, friction factors and patterns of fluid flow using the oil-lampblack technique. They stated large enhancements of the mass/heat transfer coefficient with accompanying large pressure drops.

Han and Park [6] determined the distribution of the local mass/heat transfer coefficient in a short rectangular channel with a pair of opposite rib-rough-

NOMENCLATURE

A	total transfer surface area	$j_{M,i}$	mean Chilton–Colburn factor for mass transfer for the i th segment of the duct, $St_{M,i}Sc^{2/3}$
A_S	transfer surface area for the segment	L	length of the segment
A', A''	cross-section area of the plenum and of the segment of the duct, respectively	L_0	overall length of the duct
c_p	specific heat at constant pressure	n	valence change of reacting ions
C_b	bulk concentration of ferricyanide ions [kmol m^{-3}]	p	pressure
CR	contraction ratio, A'/A''	P	pumping power
d	diameter of segments	Pr	Prandtl number
d^*	equivalent diameter for the duct, $A/(\pi L_0)$	PR	rib pitch-to-rib height ratio [10]
DR	displacement ratio, e/d	Re	Reynolds number, wd/ν
e	displacement of neighbouring segments	Re^*	reduced Reynolds number for periodic duct, $Re d/d^*$
f	friction factor, $\Delta p/[(\rho w^2/2)(L_0/d)]$	Sc	Schmidt number
F	Faraday constant, $96493 \cdot 10^3 \text{ As kmol}^{-1}$	St_M	Stanton number for mass transfer mean for the whole duct, h_D/w
h_D, h_H	mean for the whole duct mass and heat transfer coefficient, respectively	$St_{M,i}$	Stanton number for mass transfer mean for the i th segment of the duct, $h_{D,i}/w$
$h_{D,i}$	mean mass transfer coefficient for the i th segment of the duct (2)	St_H	Stanton number for heat transfer for the whole duct, $h_H/(c_p \rho u)$
I_p, i_p	plateau current and plateau current density, respectively	u	velocity of the heat transferring fluid
j_M, j_H	mean value of the Chilton–Colburn factor for the whole duct for mass and heat transfer, respectively	w	mean velocity of electrolyte in the segment of the duct
j_M^*	reduced mean Chilton–Colburn factor for the whole duct for mass transfer, $h_D/(w^* Sc^{2/3})$	w^*	reduced mean velocity of electrolyte, $w(d/d^*)^2$
$j_{M,SM}$	j_M factor for the Sparrow and Molki research [1]	x_i	mean axial position of the i th-cathode.
		Greek symbols	
		α	conic angle
		ν	kinematic viscosity
		ρ	density
		ψ	performance factor, equation (27).

ened walls changing the rib-angle-of-attack and channel aspect ratio. Semi-empirical correlations obtained made it possible for the results to be used in the design of turbine blade cooling channels.

In the light of the above literature survey, the reported research contributes to the present knowledge of the relevant technical information on forced convection for unconvective short ducts in the presence of the plenum-like space upstream of the inlet. For the applied electrolytic technique, the presented mass transfer results can be used for convective heat transfer, in effect, with the thermal boundary condition of uniform wall temperature, by means of the mass–heat transfer analogy.

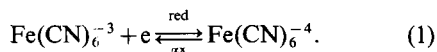
A typical engineering application of the short ducts, with the plenum upstream of the inlet, is that for the cooling of turbine blades. This type of cooling is suitable for stages with a comparatively lower working gas turbine. The configuration of ducts discussed in this paper is rather simple in the context of the above-mentioned application. It should not appear as essen-

tial obstacles regarding their producibility. The filler from the high-temperature alloy can be removed from the inside of the forged blades by the base etching. The plenum-like volume also appears in a cooler and heater of a Stirling engine at the inlet of the working gas to usually round smooth tubes. Intensifying the heat transfer by replacing the tubes, by ones examined here, reduces the overall dimensions and the weight of the engine. A similar situation also exists in flow calorimeters for measurements of the gas–fuel calorific value.

EXPERIMENTAL TECHNIQUE

The well known diffusion-controlled electrolytic technique [7] was used in the experiment. The reacting ions were: $\text{Fe}(\text{CN})_6^{3-}$ and $\text{Fe}(\text{CN})_6^{4-}$ appearing in equimolar quantities. A 1 M water solution of NaOH served as a basic electrolyte, so migration of the reacting ions could be neglected. The rule of convection of the ions to the surface of the electrode was also

insignificant in the conditions of the experiment. The only substantial mechanism of mass exchange was diffusion. The reaction occurring was



As the surface area of the cathode was much smaller than that of the anode, the limiting-current was cathode-controlled, and the concentration of ferricyanide ions was measured using iodometric titration. The temperature of the electrolyte was 25°C, so the basic data used for the calculations were [8]: $\rho = 1040 \text{ kg m}^{-3}$, $\mu = 1.11 \times 10^{-3} \text{ kg m}^{-1} \text{ s}^{-1}$ and $D = 6.71 \times 10^{-10} \text{ m}^2 \text{ s}^{-1}$. It is obvious that for the above reaction

$$h_{D,i} = I_p / (nFA_s C_b) = 2.196 \times 10^{-6} i_p / C_b. \quad (2)$$

A more detailed description of the experimental technique with comprehensive discussion of the essential physical properties of the electrolyte, including errors, relevant literature, and the principles on which the technique is based, are given in ref. [8].

APPARATUS

The rig used, presented in Fig. 1, was basically the same as that in ref. [8]. The automatic device, presented there, enabled the polarization curves to be recorded automatically. It consisted of the following instruments:

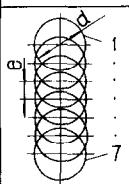
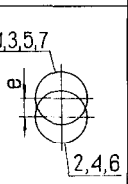
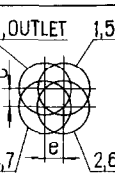
- **CONTROLLER**—special electronic device for automatic input governing of the step-increasing voltage (increments: 0.025 and 0.1 V) in the range of 0–2.5 V every t s (continuous regulation of t in the range of 4–13 s), the prototype was designed in Rzeszów University of Technology;
- **PRINTER**, type ERD-102, KFAP-Kraków, Poland, for voltage and current printing;
- **LINE RECORDER**, type TZ 4100, Czechoslovakia, for polarization—curves recording.

- **DVM**, type V541, Mera-Tronik, Poland, for measuring the temperature of an electrolyte and for controller verification.

The scheme of the test section used is shown in Fig. 2. The electrolyte entered the duct after passing the diffuser ($\alpha = \pi/18$) and the plenum ($\text{CR} = 16$, $L'/d' = 2.14$). The test section consisted of seven cylindrical segments ($d = 17 \text{ mm}$, $L/d = 1.177$) positioned in three different modes depicted in Table 1. The displacement value e was constant for all three configurations. Segments of Duct I were positioned in a step-array, and of Duct II in an alternate step-array, having their axes in the same plane. In turn, the configuration of Duct III was whirly with alternate steps. For all ducts; $e = 6 \text{ mm}$ and $\text{DR} = 0.353$. The nickel segments—cathodes were electrically isolated from each other by thin rubber. The wall thickness of the segments was 6 mm, so that total transfer surface area comprised of the surface area of all circular cut-outs perpendicular to the axes except the area of annular surface at the inlet to the duct, which was covered by eraldite. The overall length of the test sections to diameter ratio was $L_0/d = 8.24$.

The cylindrical anode, having a working surface area much greater than that of the test section, was placed downstream of the cathodes. Pressure taps

Table 1. Configurations of ducts

DUCT	I	II	III
SCHEME & SEGMENT NO.	1 2 3 4 5 6 7	1 2 3 4 5 6 7	1 2 3 4 5 6 7
CONFIGURATION			

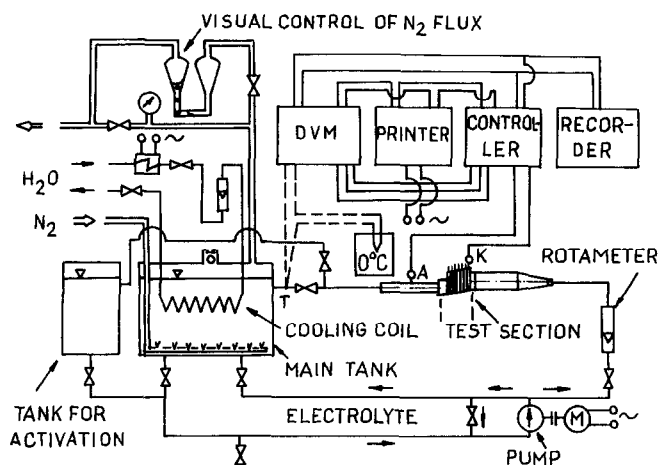


Fig. 1. Scheme of the rig.

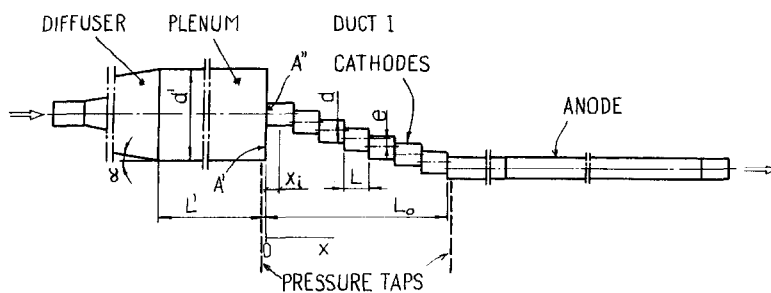


Fig. 2. Test section.

were used for overall pressure loss measurements. The tap situated downstream of the test section was designed as a collector.

Great care was taken for the correct preparation of nickel surfaces of particular segments of the test section and of the anode. Eventually, they were polished with diamond paste 1/0 and neutral paste containing chalk. They were finally rinsed with CCl_4 to avoid the presence of any grease on them, and washed with distilled water. The nickel used contained the following contaminations in percentages: Fe—0.198, Co—0.105, Cu—0.052, Mg—0.0015, Mn < 0.0015, Si < 0.005.

MEASUREMENTS AND THEIR RESULTS

The research was carried out in three cycles, in the following order: Duct I, II and III. Each cycle consisted of the preparation of the section, cathodes-activation, preliminary tests, measurements and elaborating of the results.

The aim of activation of the cathodes was to get low values of voltage for the beginning of controlled-diffusion and, thanks to that, a long plateau of the polarization-curve. Cathodes were activated individually with the use of a 5 M water solution of

NaOH. The current density applied was 20 mA cm^{-2} and the work-time of each segment was 55 min.

Preliminary tests for mass transfer following the activation, carried out with the use of the working electrolyte, resulted in the stabilization of, at first, slightly increasing mass transfer coefficients. The tests lasted 175 min for each cathode of Duct I and were somewhat shorter for Ducts II and III.

The polarization-curves obtained for each cathode were of very good quality in the entire range of Re . One can see it in Fig. 3, which presents an example for cathode no. 6 of Duct I. Fragments of the curves corresponding to the controlled diffusion are horizontal and distinctive even for the highest value of Reynolds number.

After preliminary tests for each duct, two main measurements of mass transfer and pressure drop were conducted in an interval of three days. The pressure drops measurements were made with the help of an ordinary U-tube manometer. The ferricyanide ion concentrations, measured by iodometric titration, were relatively high and constant during the whole runs. The results of the two measurements for each duct were almost identical. The arithmetic mean of the two results was calculated for further elaboration.

For the purpose of using the results in solving both

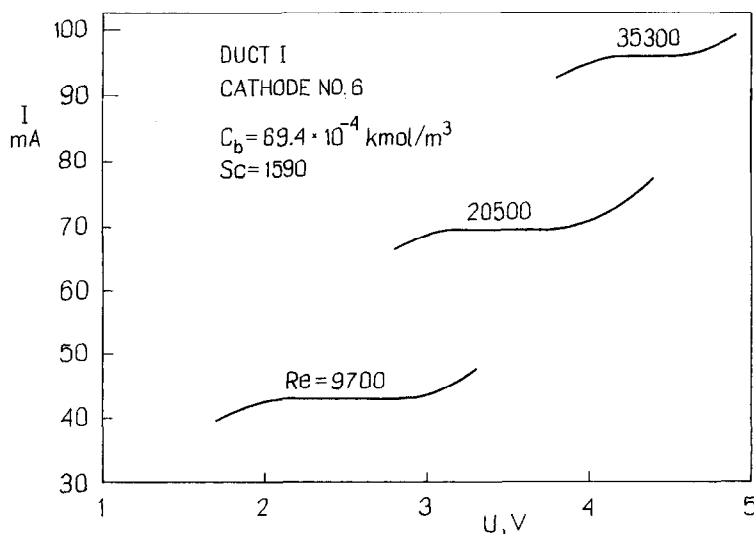


Fig. 3. Example of polarization-curves.

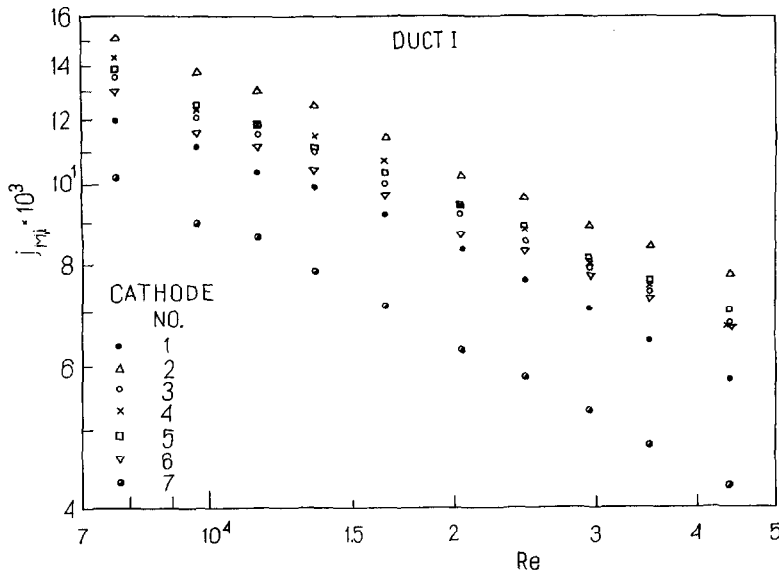


Fig. 4. Results of experiments as $j_{M,i}$ -factor vs Re .

mass and heat transfer problems, the very well known Chilton–Colburn analogy [9] was utilized, according to which :

$$j_M = St_M Sc^{2/3} \tag{3}$$

$$j_H = St_H Pr^{2/3} \tag{4}$$

$$j_M = j_H. \tag{5}$$

The assessment of the uncertainties associated with the results of electrolytic mass transfer measurements, based on a detailed uncertainty analysis, is presented in ref. [8]. It is also entirely valid in this case.

The mean values of the j -Chilton–Colburn mass transfer coefficient for particular cathodes vs Reynolds number are presented by points in Figs. 4–6, where Re is based on the inside diameter of segments d . The change of $j_{M,i}$ with Re is rather typical. The

same results may be seen in Figs. 7–9 as $j_{M,i}$ along the duct at parameter Re . These graphs, presenting variable boundary conditions, are of peculiar importance for temperature distribution in the walls of the ducts.

What is remarkable is that the shape of the curves in Fig. 9 is in contrast to that in Figs. 7 and 8, which one may try to explain by fact of the existence of a whirl during the flow of the electrolyte through Duct III.

Mean values of j_M factor vs Re for Ducts I, II and III can be seen in Fig. 10. The mean square error of the presented correlations was assessed as equal to 17%. Additionally, for comparison, two correlations are also presented for short ducts with similar inlet configurations. The first one, for the plane tube with the baffle plate at the inlet, has been constructed with the help of data obtained by use of the sublimation

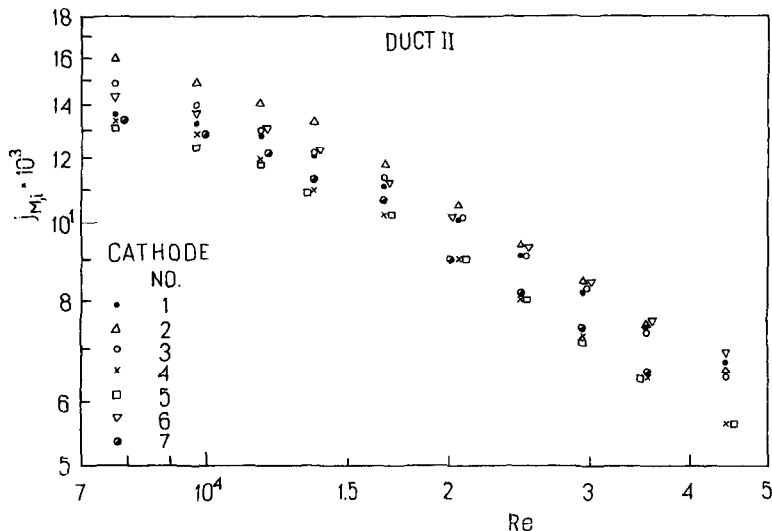


Fig. 5. Results of experiments as $j_{M,i}$ -factor vs Re .

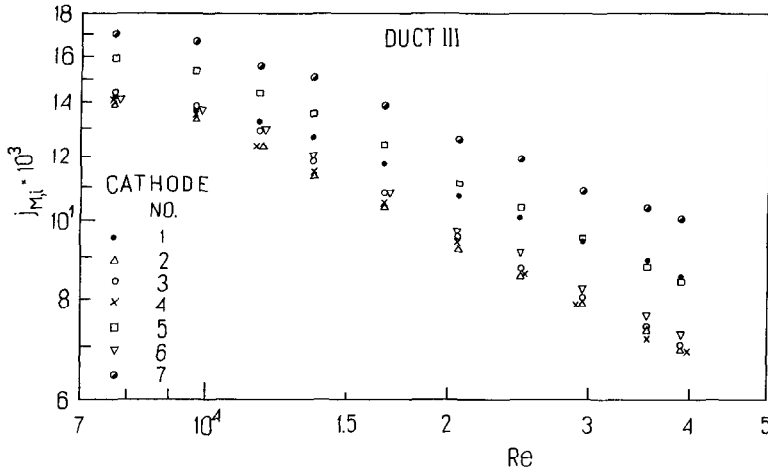


Fig. 6. Results of experiments as $j_{M,i}$ -factor vs Re .

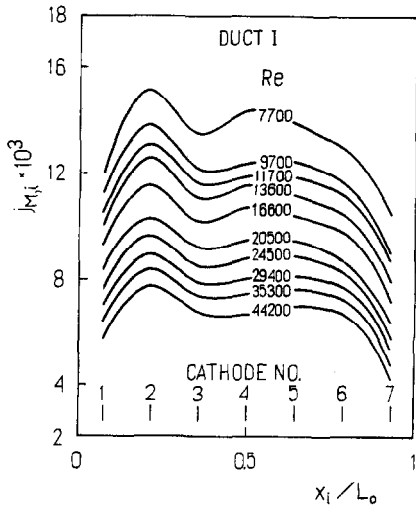


Fig. 7. Distribution of $j_{M,i}$ -factor along the duct.

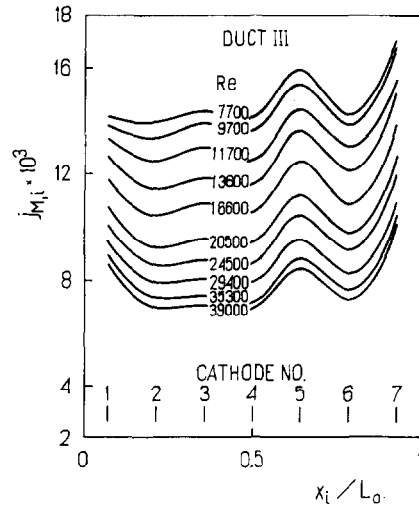


Fig. 9. Distribution of $j_{M,i}$ -factor along the duct.

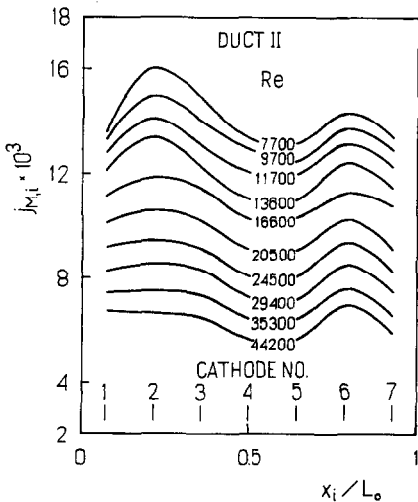


Fig. 8. Distribution of $j_{M,i}$ -factor along the duct.

technique, published in ref. [1] (Fig. 2). The data were transformed to the j_M -factor by planimetry for $L_0/d = 8.24$ and use of the Chilton–Colburn analogy for $Sc = 2.5$, as in the above-mentioned experiment. The second one, for the rectangular duct with the plenum at the inlet and repeated square-rib pairs on the two opposite walls, at rib height-to-duct height ratio equal 0.13, was constructed with help of equation (7) in ref. [10]. The results were obtained by use of laser holographic interferometry in a thermal experiment. The data on the average Nusselt numbers, for rib pitch-to-rib height ratio equal to 10, were transformed to the j_H factor by use of the Chilton–Colburn analogy for $Pr = 0.7$.

Friction losses can be seen in Fig. 11. They are comparable for Ducts I and II at $Re > 14000$, whereas at lower values of Re predominance of the Duct II is distinct. The friction factor for Duct III is considerably greater than that for Duct II, e.g. about

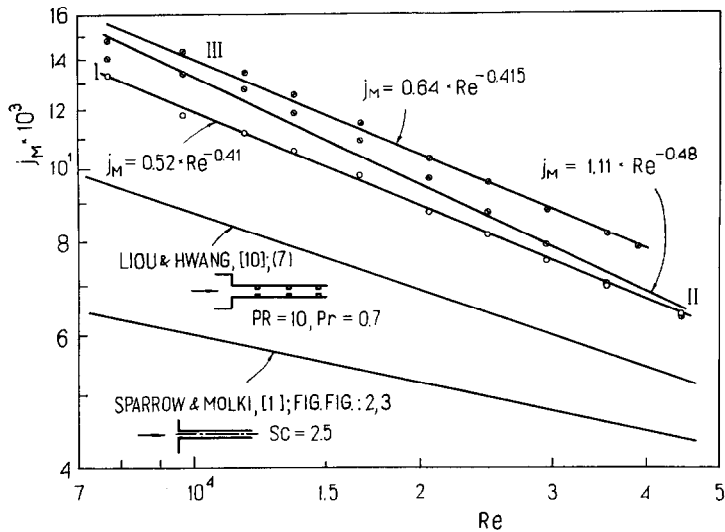


Fig. 10. Mean value of j_M -factor for the whole duct and appropriate correlations.

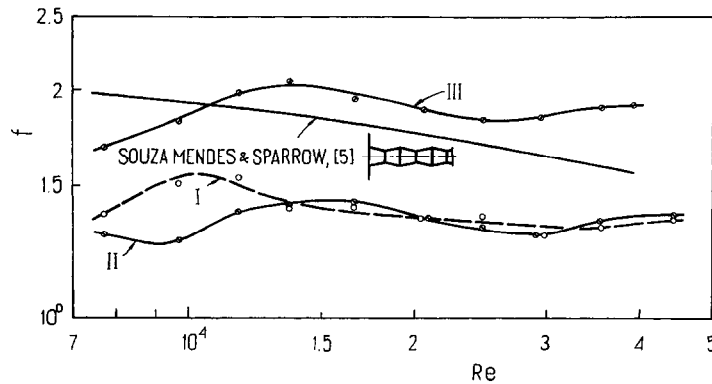


Fig. 11. Friction losses for the whole duct.

30% at $Re = 7700$ and 40% at $Re > 9700$. Supposed occurrence of the screw-motion of fluid in the case of Duct III might serve as an explanation of the result obtained.

The fourth curve presents one of the results, for fully-developed friction factors, published [5] for a periodic tube consisting of conical converging and diverging modules built into a large baffle plate. The curve concerns the following data: module aspect ratio $L_{mod}/D_{max} = 1.143$ and half taper angle $\theta = 14.8^\circ$. In this case, separation of flow at the inlet to the duct took place as well. The comparison convinces one that despite the sharp edges and the whirl in Duct III, its friction loss characteristic is close to that of the last duct.

PERFORMANCE ANALYSIS

The performance analysis [5] enables quantitative answering to the question of whether or not to employ the duct in practical applications. Usually, one undertakes comparisons of a duct with the plane one. The procedure takes into account mass (heat) transfer coefficients as friction factors for constraints appro-

appropriate to a foreseen application. Commonly applied constraints at equal transfer surface area for the two ducts are:

- (1) equal flow rate without considering the flow friction power (Case 1);
- (2) equal pumping power at different flow rates (Case 2);
- (3) equal flow rate with considering the flow friction power (Case 3).

Case 1

For this case the mean mass (heat) transfer Chilton-Colburn coefficients for a short periodic duct and for a short straight plane tube, both at the same length to equivalent diameter ratio, at similar inlet configuration (i.e. plenum and baffle plate, respectively) will be evaluated for comparison with each other.

The common constraint of equal transfer surface area may be fulfilled by applying to the short periodic duct the equivalent diameter equal

$$d^* = A/(\pi L_0) \quad (6)$$

where A means the total transfer surface area of the

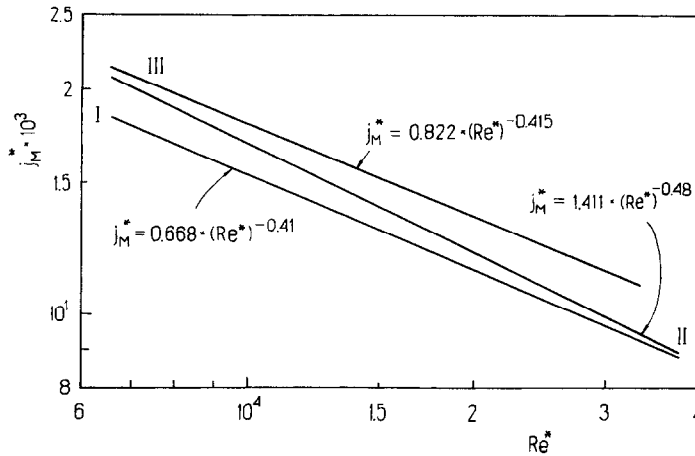


Fig. 12. Reduced correlations obtained by the use of the equivalent diameter.

duct, and comparing a periodic tube with a straight plane tube of the same diameter. In this work, d^* slightly exceeds d , as the areas of surfaces perpendicular to the duct axis were added to the areas of cylindrical surfaces, $d^*/d = 1.171$.

For the purpose of Case 1 comparison, Reynolds numbers and j -factors were reduced to

$$Re^* = w^* d^* / \nu \tag{7}$$

and, according to the Chilton–Colburn analogy, to

$$j_M^* = h_D / (w^* Sc^{2/3}) \tag{8}$$

by means of the following expressions:

$$Re^* = Re(d/d^*) \tag{9}$$

valid for incompressible fluid, and

$$j_M^* = j_M (d^*/d)^2. \tag{10}$$

The results of the reduction are depicted in Fig. 12, in which correlations stated for the three ducts are given. They indicate that mass/heat transfer in Duct II is for $Re = 7000$ at about 14% and for $Re = 37500$ at 1% more intensive than in Duct I. Relative increase of mass/heat transfer coefficient for Duct III in com-

parison to Duct I equals about 17% in the whole range of Reynolds numbers.

Comparison of the reduced results with the data of Sparrow and Molki [1], for a round tube with a built-in inlet, for $L_0/d = 8.24$, is presented in Fig. 13. The result for Duct I here is almost identical with the naphthalene-sublimation result of Souza Mendes and Sparrow, presented in ref. [5] (Fig. 7), for a periodic tube consisting of conical converging and diverging modules built into a large baffle plate at module aspect ratio $L_{mod}/D_{max} = 0.762$ and 1.143 for half taper angle $\theta = 10^\circ$, and per cycle fully developed mass/heat transfer coefficient (depicted in Fig. 13 by a dashed line).

Case 2

Attention may now be directed to Case 2 of the performance analysis, i.e. at equal transfer surface area and pumping power. The enhancement in mass (heat) transfer coefficient as a result of flow turbulence usually occurs at a simultaneous increase of associated pressure drop. That is why additional performance analysis at constant pumping power and equal transfer surface area is necessary. The analysis

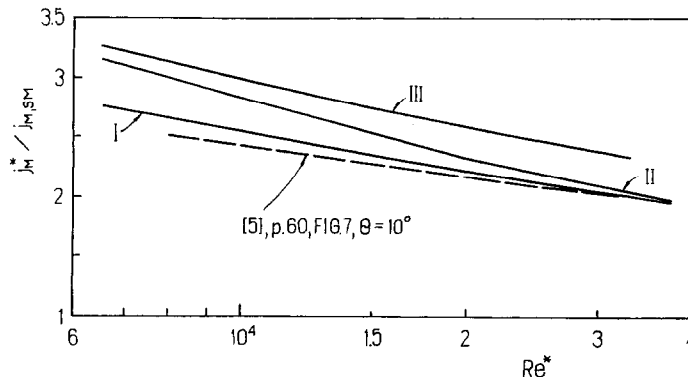


Fig. 13. Results of the performance analysis by comparison with the cylindrical duct; Case 1—at equal surface area and equal flux.

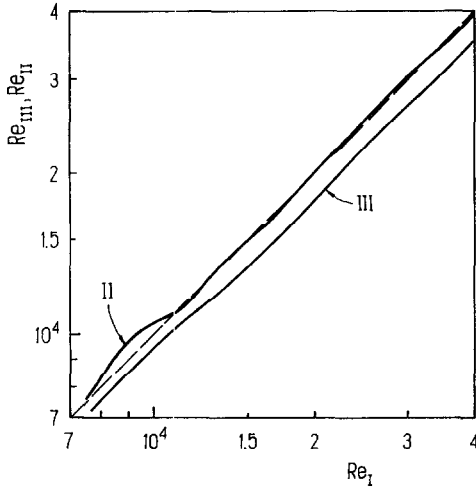


Fig. 14. Correlation between Reynolds numbers for ducts working at the same heat transfer surface area and the same pumping power; Case 2.

was done for Ducts III and II in comparison with Duct I.

During the duct flow of fluid of density ρ , at a flow rate \dot{m} and pressure drop Δp , the pumping power is

$$P = \dot{m} \Delta p / \rho. \quad (11)$$

Equalizing the pumping power for Duct I with the pumping powers of Ducts III and II yields

$$(\dot{m} \Delta p / \rho)_I = (\dot{m} \Delta p / \rho)_{III} \quad (12)$$

and

$$(\dot{m} \Delta p / \rho)_I = (\dot{m} \Delta p / \rho)_{II}. \quad (13)$$

Putting into the above equations:

$$\dot{m} / \rho = w A'' \quad (14)$$

$$\Delta p = f(\rho w^2 / 2)(L_0 / d) \quad (15)$$

$$w = Re v / d \quad (16)$$

yields

$$f_I Re_I^3 = f_{III} Re_{III}^3 \quad (17)$$

$$f_I Re_I^3 = f_{II} Re_{II}^3. \quad (18)$$

Re instead of Re^* is used in the above equations because the transfer surface areas for all the ducts are equal.

The equations concern the dependence between the Reynolds numbers for different ducts at equal pumping power. Let us compare Duct III with Duct I. For a certain value of Re_I , f_I may be read from Fig. 11. From the same figure $f_{III,1}$ may be read approximately. The first approximation

$$Re_{III,1} = \sqrt[3]{f_I / f_{III,1}} Re_I. \quad (19)$$

The value of f_{III} read from Fig. 11 for $Re_{III,1}$ differs slightly from $f_{III,1}$, so the second approximation was made in order that $f_{III,2}$, read in Fig. 11, and $Re_{III,2}$

fulfil equation (17). Results obtained in this way for Ducts III and II, in comparison with Duct I, are plotted in Fig. 14, in which the dashed line corresponds to an equal Reynolds number. It can be seen, that Duct III must work at lower Reynolds numbers than Duct I at equal pumping power.

On the basis of the just determined Reynolds number relations, j_M factors for all the short ducts were determined from the correlations given in Fig. 10. The factors were ratioed and plotted in Fig. 15. From the last figure results the distinct superiority of Duct III over Ducts II and I (dashed line).

Case 3

The objective of the analysis in Case 3 at equal surface area and flow rate, considering the flow friction losses, is making it possible for the choice of the optimal duct to be made using a criterion of relative overall heat conductance $h_H A$ per relative convectional rate of pumping costs.

One can derive, on the basis of the Newton's equation for convection, that the overall heat conductance

$$h_H A = \frac{\pi}{4} \mu c_p Re St_H A \quad (20)$$

which, after applying equations (4) and (5) yields

$$h_H A = C_1 Re j_M A \quad (21)$$

where

$$C_1 = \frac{\pi}{4} \mu c_p Pr^{-2/3}. \quad (22)$$

Then from equation (11) and (14)–(16) one gets

$$P = C_2 A f Re^3 \quad (23)$$

where

$$C_2 = \frac{\rho}{8} \left(\frac{v}{d} \right)^3. \quad (24)$$

Eliminating Re from equations (21) and (23), for equal flow rate, yields

$$C_3^{1/3} \frac{h_H A}{P^{1/3} A^{2/3}} = \frac{j_M}{f^{1/3}} \quad (25)$$

where

$$C_3 = C_2 / C_1^3 = \frac{8}{\pi^3} \left(\frac{Pr}{\rho} \right)^2 \frac{1}{(c_p d)^3}. \quad (26)$$

Using (25) for comparison of Duct III and II with Duct I results in the performance factor

$$\Psi \equiv \frac{h_H A / (h_H A)_I}{(P/P_I)^{1/3} (A/A_I)^{2/3}} = \frac{j_M / j_{M,I}}{(f/f_I)^{1/3}} \equiv \frac{St_M / St_{M,I}}{(f/f_I)^{1/3}} \quad (27)$$

which, for the same surface area, after applying the Chilton–Colburn analogy [equations (3)–(5)], yields

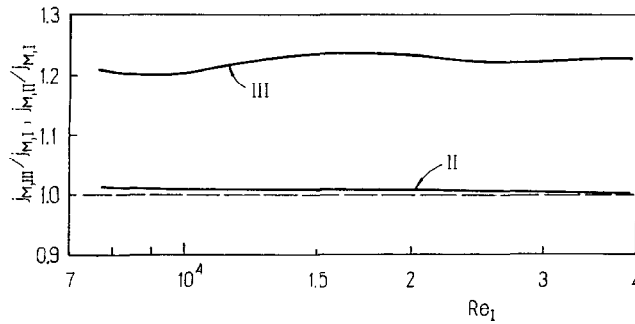


Fig. 15. Results of the performance analysis by comparison with the ducts; Case 2—at equal heat transfer surface area and equal pumping power.

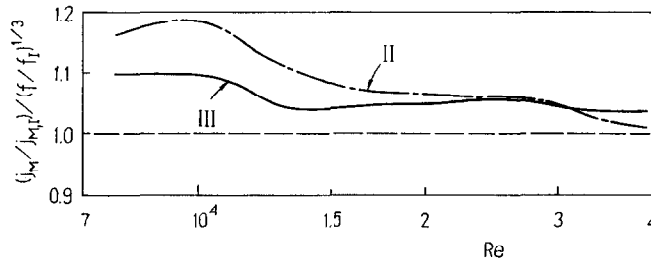


Fig. 16. Relative thermal performance coefficient for Duct III and II obtained by comparison with Duct I at equal heat transfer surface area and equal flow rate.

$$\Psi = \frac{St_H/St_{H,I}}{(f/f_I)^{1/3}} \quad (28)$$

compared to equation (5) in ref. [11].

The effects of using equation (27) for performance factor calculations are presented in Fig. 16 and show the predominance of Duct III and II over Duct I. Duct II dominates over Duct III for lower Re ; for higher Re the performances of the both ducts are approximately the same.

CONCLUSIONS

The work concerned the search on three different short ducts with regard to convective mass/heat transfer and friction. The ducts consisted of seven cylindrical segments and were preceded by the plenum. An electrolytical technique was used for measurement of the mass/heat transfer coefficient. Experiments were carried out at the same length of segments, displacement ratio and contraction ratio. The parameter which was varied was the Reynolds number.

(1) Distribution of the mass/heat transfer coefficient which was mean for each segment, along ducts, and pressure losses for whole ducts vs Re , were determined.

(2) Comparison of the mean mass/heat transfer coefficient for the entire short Ducts I, II and III with those for smooth [1] and periodic tube [5], and also for the rectangular ribbed duct of certain geometry [10] is an advantage for the ducts under consideration.

(3) Correlations for mean mass/heat transfer

reduced j_M^* factor for all ducts were stated with the use of equivalent diameter of ducts as follows:

$$j_M^* = 0.668 Re^{*-0.41} \text{ for Duct I}$$

$$j_M^* = 1.411 Re^{*-0.48} \text{ for Duct II and}$$

$$j_M^* = 0.822 Re^{*-0.415} \text{ for Duct III.}$$

The reduced j_M^* factor for Duct III, at the same transfer area, and at equal flow rate, which is the highest one, is about 17% higher than that of Duct I.

(4) Mean j_M factor for Duct III is more than 1.2 times higher than that of Duct I at the same pumping power in the entire range of Re_I .

(5) The performance factor, in the case of equal surface area and equal flow rate considering the flow friction losses, is higher for Duct II in the range of lower Re , being almost equal to that for Duct III at higher Reynolds numbers.

(6) The above-mentioned advantageous performances may encourage the designers to apply simple Ducts II and III for the convective cooling of short elements of thermal machines, e.g. blades of, especially, the last but one gas turbine stages.

Acknowledgements—The author would like to acknowledge the help of mgr inż. Joanna Wilk and mgr inż. Krzysztof Kiedrzyński in realization of the work.

REFERENCES

1. Sparrow, E. M. and Molki, M., Turbulent heat transfer coefficients in an isothermal-walled tube for either a

- built-in or free inlet. *International Journal of Heat and Mass Transfer*, 1934, **27**, 669–675.
2. Dutra, A. S., Souza Mendes, P. R. and Parise, J. R., Transport coefficients for laminar and turbulent flow through a four-cusp channel. *International Journal of Heat and Fluid Flow*, 1991, **12**, 99–105.
 3. Sparrow, E. M. and Cur, N., Maldistributed inlet flow effects on turbulent heat transfer and pressure drop in a flat rectangular duct. *Transactions of the ASME, Journal of Heat Transfer*, 1983, **105**, 527–535.
 4. Goldstein, Jr, L. and Sparrow, E. M., Heat/mass transfer characteristics for flow in a corrugated wall channel. *Transactions of the ASME, Journal of Heat Transfer*, 1977, **99**, 187–195.
 5. Souza Mendes, P. and Sparrow, E. M., Periodically converging–diverging tubes and their turbulent heat transfer, pressure drop, fluid flow, and enhancement characteristics. *Transactions of the ASME, Journal of Heat Transfer*, 1934, **106**, 55–63.
 6. Han, J. C. and Park, J. C., Developing heat transfer in rectangular channels with rib turbulators. *International Journal of Heat and Mass Transfer*, 1988, **31**, 183–195.
 7. Eisenberg, M., Tobias, C. W. and Wilke, C. R., Ionic mass transfer and concentration polarization at rotating electrodes. *Journal of Electrochemical Society*, 1954, **101**, 306–318.
 8. Bieniasz, B. and Wilk, J., Forced convection mass/heat transfer coefficient at the surface of the rotor of the sucking and forcing regenerative exchanger. *International Journal of Heat and Mass Transfer*, 1995, **38**, 1823–1830.
 9. Chilton, T. H. and Colburn, A. P., Mass transfer (absorption) coefficients prediction from data on heat transfer and fluid friction. *Industrial Engineering and Chemistry*, 1934, **26**, 1183–1187.
 10. Liou, Tong-Miin and Hwang, Jenn-Jiang, Developing heat transfer and friction in a ribbed rectangular duct with flow separation at inlet. *Transactions of ASME, Journal of Heat Transfer*, 1992, **114**, 565–573.
 11. Webb, R. L. and Eckert, E. R. G., Application of rough surfaces to heat exchanger design. *International Journal of Heat and Mass transfer*, 1972, **15**, 1647–1658.